

RESEARCH MEMORANDUM

INTERNAL PERFORMANCE AT MACH NUMBERS TO 2.0 OF TWO
AUXILIARY INLETS IMMERSED IN FUSELAGE
BOUNDARY LAYER

By Donald B. Pennington and Paul C. Simon

Lewis Flight Propulsion Laboratory
Cleveland, Ohio

NATIONAL ADVISORY COMMITTEE
FOR AERONAUTICS
WASHINGTON

March 10, 1954
Declassified February 10, 1959

NATIONAL ADVISORY COMMITTEE FOR AERONAUTICS

RESEARCH MEMORANDUM

INTERNAL PERFORMANCE AT MACH NUMBERS TO 2.0 OF TWO AUXILIARY

INLETS IMMERSED IN FUSELAGE BOUNDARY LAYER

By Donald B. Pennington and Paul C. Simon

SUMMARY

An experimental investigation was conducted to evaluate the internal performance of two types of auxiliary air inlets, a submerged and a scoop inlet, operating within the turbulent boundary layer existing on the bottom of a typical supersonic fighter aircraft afterbody. Diffuser-exit total-pressure recovery and mass flow were obtained at stream Mach numbers of 0.64 and from 1.5 to 2.0 at angles of attack of 0 and 3°.

The maximum total-pressure recovery of the submerged inlet was 0.35 and 0.17 at stream Mach numbers of 1.5 and 2.0, respectively. At these same Mach numbers the scoop inlet critical recovery, 0.45 and 0.27, fell considerably below the theoretically possible values.

INTRODUCTION

In addition to the engine air-flow requirements of power plants for supersonic vehicles, auxiliary air may be needed for engine cooling and accessory drive purposes. This auxiliary air may be furnished by the engine air source or, in some cases, by one or more independent auxiliary inlets.

Although considerable effort has been expended in studying the performance of jet-engine air inlets, little is known about the performance of small, independent auxiliary inlets. The size, type, and location of the auxiliary inlet will vary with the weight flow and pressure level required. Since the weight-flow and pressure-level requirements are usually low, compared with the engine, and since the installed drag should be kept to a minimum, it may be necessary to place such auxiliary inlets within the fuselage or the wing boundary layer.

An investigation was therefore undertaken, utilizing an existing model, to evaluate the internal performances of both a submerged and a scoop auxiliary inlet. These inlets were operated in the turbulent boundary layer existing on the bottom of the aft section of a typical supersonic fighter aircraft fuselage.

The investigation was conducted in the NACA Lewis 8- by 6-foot supersonic wind tunnel at Mach numbers of 0.64 and from 1.5 to 2.0 and at angles of attack of 0 and 3°. Reynolds number, based on model length ahead of the inlet and free-stream conditions, varied between 15×10^6 and 19×10^6 .

SYMBOLS

The following symbols are used in this report

A area, measured perpendicular to duct center line, sq in.

a inlet lip height: for submerged inlet, 0.27 in.;
for scoop inlet, 0.60 in.

M_δ local Mach number outside boundary layer

M_0 stream Mach number

$\frac{\bar{M}_{bl}}{M_0} = \frac{\int_0^a M dy}{M_0 a}$ ratio of area-weighted average Mach number in
boundary layer to free-stream Mach number

m mass flow

$\frac{m_2}{m_0} = \frac{m_2}{\rho_0 V_0 A_1}$ ratio of duct mass flow to mass flow in free-stream
tube equal to inlet lip area

$\frac{m_{bl}}{m_0} = \frac{\int_0^a \rho u dy}{\rho_0 V_0 a}$ ratio of mass flow in boundary layer to mass flow in
free-stream tube equal to scoop inlet lip area

P total pressure

\bar{P}_{bl} area-weighted average total pressure in boundary
layer

$$\frac{\bar{P}_{bl}}{P_0} = \frac{\int_0^a P \, dy}{P_0 a}$$

ratio of area-weighted average total pressure in boundary layer to free-stream total pressure

Re	Reynolds number, $\rho_0 V_0 l / \mu_0$ ($l = 47.83$ in.)
U_δ	local stream velocity outside boundary layer
u	velocity in boundary layer
V	velocity
X, Y, Y', Z	duct coordinate dimensions (see figs. 3 and 4)
y	distance normal to fuselage model surface
α	angle of attack, deg
δ	boundary-layer thickness (defined by $u/U_\delta = 0.99$), inlet station bl , in.
μ	viscosity
ρ	density

Subscripts:

bl	plane of boundary-layer survey
cr	critical
max	maximum
0	free-stream conditions
$1, 2, 3$	inlet stations (see fig. 2)

APPARATUS AND PROCEDURE

Two inlets were alternately installed on the afterbody of a one-tenth scale model of a typical supersonic airplane fuselage. A photograph of the installation in the NACA Lewis 8- by 6-foot supersonic tunnel, together with an enlarged view of the scoop inlet, is shown

in figure 1. The isometric views of the submerged and scoop inlets pictured in figure 2 illustrate the approximate relative heights of the boundary layer and the inlet entrance. Also indicated in figure 2 are the inlet stations, bleed-off cowl slots, inlet entrance lip shape (station 1), and diffuser-exit pressure instrumentation. Detailed drawings of the inlets are given in figures 3 and 4. The flow-area variation for both inlets is given in figure 5.

Although the submerged inlet is a small-scale version of an NACA submerged inlet, the design principles of which are discussed in reference 1, it should be noted that the ratio of inlet lip height to boundary-layer thickness has been decreased considerably from the value of the full-scale inlet.

The bleed-off cowl slots were incorporated in the design of the scoop inlet to bleed off the very low-energy air existing in the lower portion of the fuselage boundary layer. This type of slot has been found to be effective in improving scoop inlet performance (refs. 2 and 3).

Emphasis should not be placed on a comparison between the performance of the submerged and scoop inlets because the inlets are dissimilar in many ways, other than the type of entrance. A larger height to width ratio, combined with a greater height to boundary-layer thickness ratio, provides the scoop inlet with air of higher energy potential than the submerged inlet. Also, the scoop inlet is provided with a considerably more gradual area variation and lower turning angle than the submerged inlet. These differences, combined with the fact that the scoop inlet is provided with boundary-layer bleed-off slots, were expected to result in distinct advantages for the scoop inlet.

The exit area of the discharge duct was varied by longitudinal motion of a remotely controlled plug (fig. 2). At supersonic conditions the mass flow and total-pressure recovery were determined by means of static-pressure measurements at inlet station 2 and sonic flow at the duct exit. The pressure ratio necessary for choking at the duct minimum area was not reached during subsonic operation, and it was therefore necessary to utilize the measured static pressures and area ratio between inlet stations 2 and 3 to establish the mass flow and total-pressure recovery.

As a check on flow stability of the scoop inlet, a dynamic pressure pickup was connected to a wall static orifice located 1 inch upstream of inlet station 2.

RESULTS AND DISCUSSION

Boundary-Layer Flow

A boundary-layer survey was conducted to establish the character of the flow conditions ahead of the inlet. The survey was made with the inlet removed, at a longitudinal fuselage station corresponding to the entrance plane of the scoop inlet. The results of the survey are presented as nondimensional boundary-layer profiles in figure 6, boundary-layer thickness in figure 7, and ratio of boundary-layer to free-stream parameters in figure 8.

The turbulent $1/7$ -power boundary-layer profile,

$$\frac{u}{U_\infty} = \left(\frac{y}{\delta}\right)^{1/7}$$

is included in figure 6 for the purpose of comparison with the experimental survey data taken at Mach numbers of 0.64, 1.5, and 1.7. The increase in boundary-layer thickness with increasing Mach number is shown in figure 7. For general interest, the theoretical two-dimensional, turbulent boundary-layer thickness of reference 4 is also included in the figure. Agreement between this theory and experiment was realized only at a Mach number of the order of 1.5. The submerged inlet always operated within the fuselage boundary layer, as did the scoop inlet at supersonic speeds.

The relation between the stream conditions and the corresponding boundary-layer Mach number, mass flow, and total pressure is presented in figure 8 in ratio form. It should be noted that throughout this report the subscript b_l denotes the integrated quantities in the boundary layer to a height of 0.6 inch, the lip height of the scoop inlet.

Inlet Performance

The inlet mass-flow and total-pressure-recovery characteristics at angles of attack of 0 and 3° for Mach numbers of 0.64 and 1.5 to 2.0 are given in figures 9 and 10. The mass-flow-ratio values at a Mach number of 0.64, for the submerged inlet (fig. 9), extend beyond the indicated maximum theoretical mass flow ratio (based on stream conditions and inlet choking). The implicit nature of the data-reduction method inherently results in increasing errors in computing the mass-flow values at the high mass flow ratios. The values of the total-pressure recovery are, however, considered accurate.

It is interesting to note that peak total-pressure recoveries comparable to those obtained with the scoop auxiliary inlet (fig. 10) have been observed for boundary-layer-removal scoops of side inlets operating in the same range of h/δ (refs. 3 and 5).

Change in model angle of attack from 0 to 3° slightly increased both the submerged and scoop inlet total-pressure recoveries throughout the mass-flow range at all stream Mach numbers investigated. This improved pressure recovery is consistent with that observed in reference 3, for example, as the ratio of boundary-layer scoop height to boundary-layer thickness was increased, and is probably due to thinning of the boundary layer on the fuselage underside as well as reduced shock losses resulting from the lower local Mach numbers.

An estimate of the critical mass-flow spillage of the scoop inlet can be determined by taking the difference between the experimental critical mass flow ratios and the maximum available mass flow ratio calculated from the boundary-layer flow, and indicated in figure 10 by the dashed lines. No attempt was made to establish the critical spillage of the submerged inlet.

The scoop inlet exhibited stable flow (no buzz) at all conditions of operation. Although dynamic measurements were not taken, the low slope of the subcritical pressure recovery - mass flow curve of the submerged inlet suggest that it too may have been free of flow instability.

The pressure recoveries of both inlets at zero angle of attack, referenced to stream total pressure, are shown on figure 11. At a Mach number of 0.64, both inlets had total-pressure recoveries of about 0.83. Between Mach numbers of 1.5 and 2.0 the scoop inlet critical pressure recovery decreased from 0.45 to 0.27 and the maximum recoveries for the submerged inlet decreased from 0.35 to 0.17.

For comparison, the total-pressure recovery of a sharp-lip submerged inlet intended as a primary engine-air source (ref. 6) is included in figure 11. The inlet of reference 6 gave better pressure recoveries than were obtained with the submerged auxiliary inlet possibly because it captured higher-energy air and had lower subsonic diffuser losses.

Also included in figure 11 is a theoretical curve based on the theory of reference 7 which represents the optimum total-pressure recovery obtainable with a normal-shock scoop inlet operating in a turbulent 1/7-power profile boundary layer at the a/δ values of the inlet being evaluated (see fig. 7).

A more realistic evaluation of the scoop inlet efficiency can be made if, instead of referring the diffuser pressure recovery to free-stream total pressure, an integration of the total pressure in the boundary layer approaching the inlet is employed as the reference pressure (fig. 12). The theory of reference 7, based on the average total pressure of a $1/7$ -power boundary-layer profile, is reproduced in the figure.

The experimental pressure recoveries, in the supersonic regime, fall well below the optimum values; however, the same general trend with Mach number is indicated. The difference between theory and experiment is an indication of additional losses, not accounted for by the theory, occurring ahead of the scoop and in the diffuser duct.

SUMMARY OF RESULTS

An investigation was conducted on a submerged auxiliary inlet and a scoop auxiliary inlet which were installed within the turbulent boundary layer on the afterbody of a typical supersonic fighter airplane. The internal performance of these inlets operating at stream Mach numbers of 0.64 and from 1.5 to 2.0 can be summarized as follows:

1. Pressure recoveries at a Mach number of 0.64 were essentially the same for both inlets. At Mach numbers of 1.5 and 2.0 and zero angle of attack, the maximum total-pressure recoveries of the submerged inlet were 0.35 and 0.17, respectively. For the same Mach numbers the scoop inlet critical recoveries were 0.45 and 0.27.

2. Change in model angle of attack from 0 to 3° increased slightly the total-pressure recovery of both the submerged and scoop inlets.

3. Because most of the air handled by the auxiliary submerged inlet is taken from the fuselage boundary layer, the pressure recovery of this inlet falls considerably below that obtained with submerged inlets intended to supply the engine mass-flow requirements.

4. The experimental pressure recovery of the scoop inlet was compared with a theory which accounts for normal shock losses of a $1/7$ -power boundary-layer profile. The theory, although optimistic in predicting the pressure recovery of the scoop inlet of this investigation, gave the same general trend of pressure recovery with stream Mach number.

5. The scoop inlet exhibited stable (no buzz) operation at all conditions investigated. Although the diffuser was not instrumented, the low slope of the subcritical mass flow - pressure recovery curve may suggest that the submerged inlet also had stable subcritical operation.

Lewis Flight Propulsion Laboratory
National Advisory Committee for Aeronautics
Cleveland, Ohio, December 28, 1953

REFERENCES

1. Sacks, Alvin H., and Spreiter, John R.: Theoretical Investigation of Submerged Inlets at Low Speeds. NACA TN 2323, 1951.
2. Davis, Wallace F., and Goldstein, David L.: Experimental Investigation at Supersonic Speeds of Twin-Scoop Duct Inlets of Equal Area. II - Effects of Slots upon an Inlet Enclosing 61.5 Percent of the Maximum Circumference of the Forebody. NACA RM A8C11, 1948.
3. Goelzer, H. Fred, and Cortright, Edgar M., Jr.: Investigation at Mach Number 1.88 of Half of a Conical-Spike Diffuser Mounted as a Side Inlet with Boundary-Layer Control. NACA RM E51G06, 1951.
4. Tucker, Maurice: Approximate Calculation of Turbulent Boundary-Layer Development in Compressible Flow. NACA TN 2337, 1951.
5. Piercy, Thomas G., and Johnson, Harry W.: A Comparison of Several Systems of Boundary-Layer Removal Ahead of a Typical Conical External-Compression Side Inlet at Mach Numbers of 1.88 and 2.93. NACA RM E53F16, 1953.
6. Anderson, Warren E., and Frazer, Alson C.: Investigation of an NACA Submerged Inlet at Mach Numbers from 1.17 to 1.99. NACA RM A52F17, 1952.
7. McLafferty, George: Theoretical Pressure Recovery Through a Normal Shock in a Duct with Initial Boundary Layer. Jour. Aero. Sci., vol. 20, no. 3, Mar. 1953, pp. 169-174.

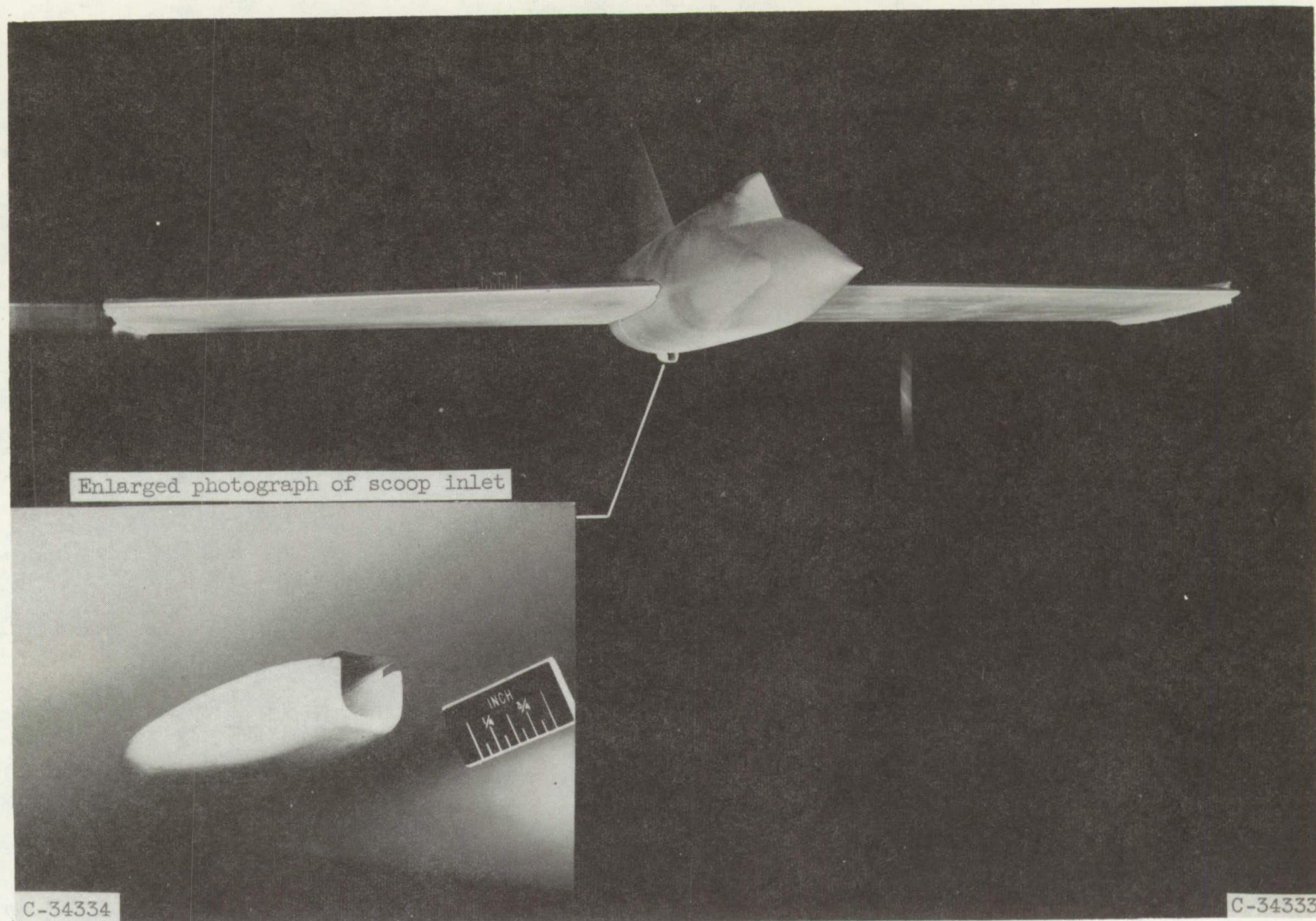


Figure 1. - Photograph of scoop inlet mounted on fuselage of primary model installed in 8- by 6-foot supersonic wind tunnel.

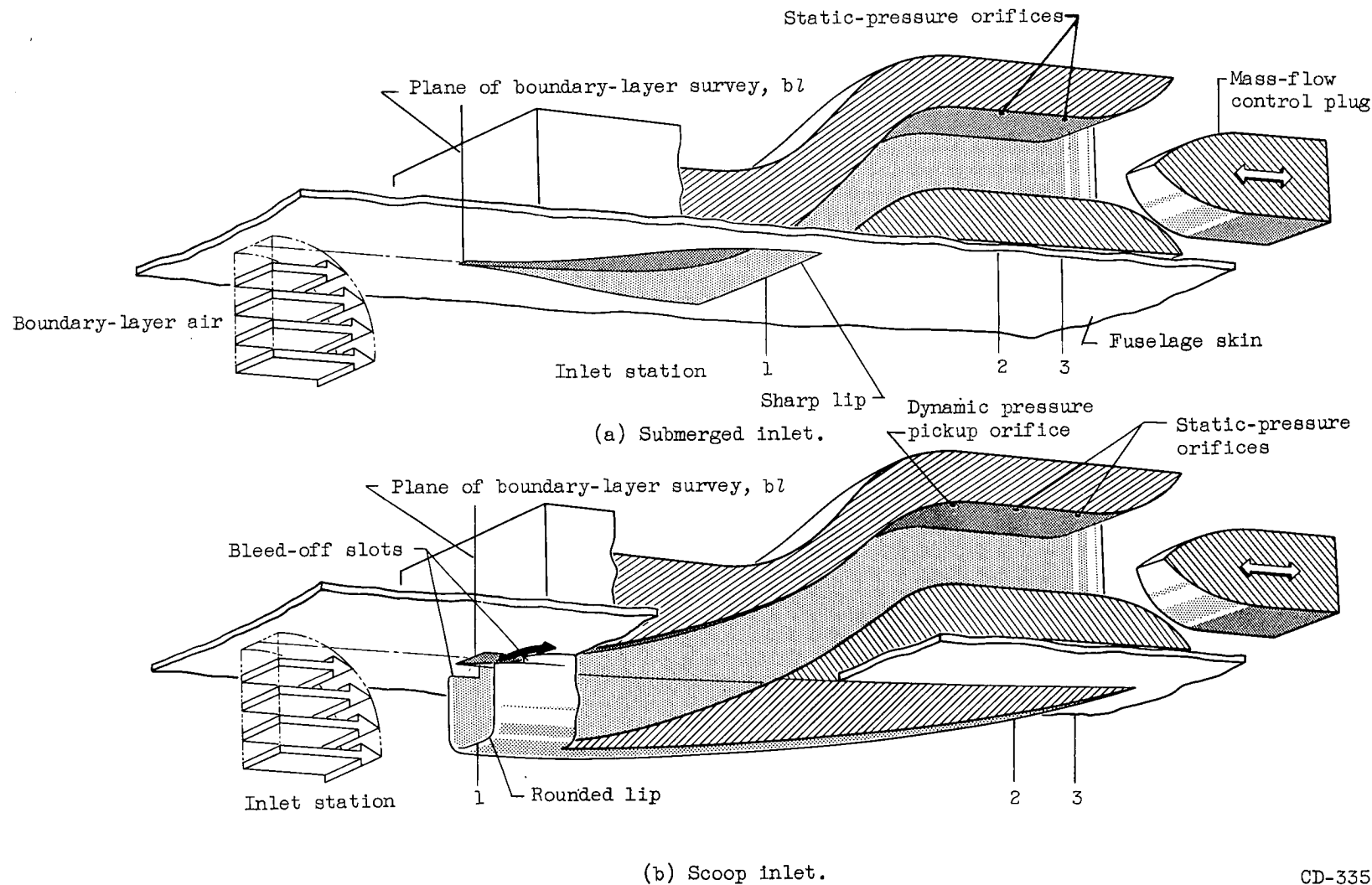


Figure 2. - Isometric views of submerged and scoop inlets.

CD-3355

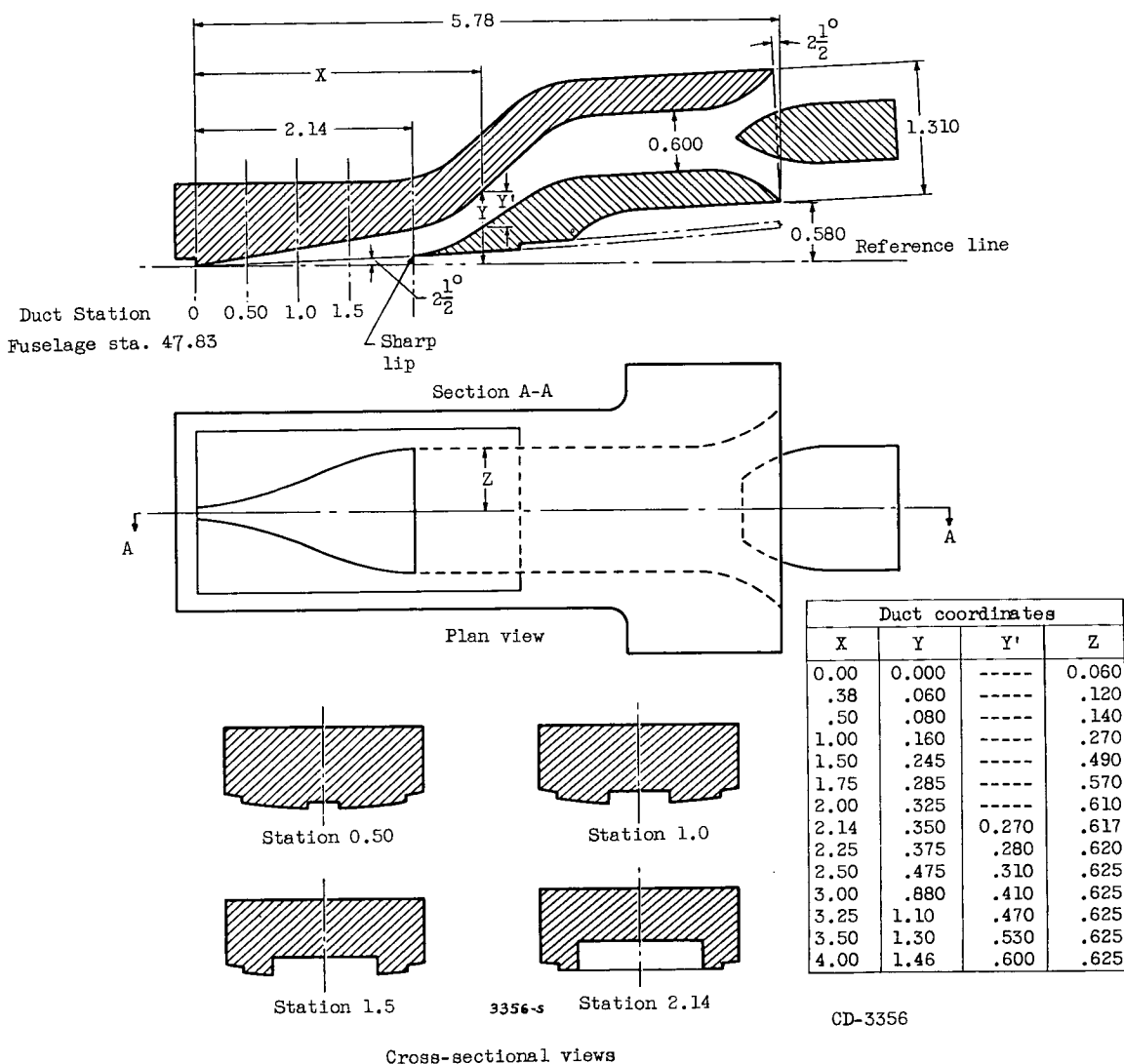


Figure 3. - Submerged inlet details. (All dimensions are in inches.)

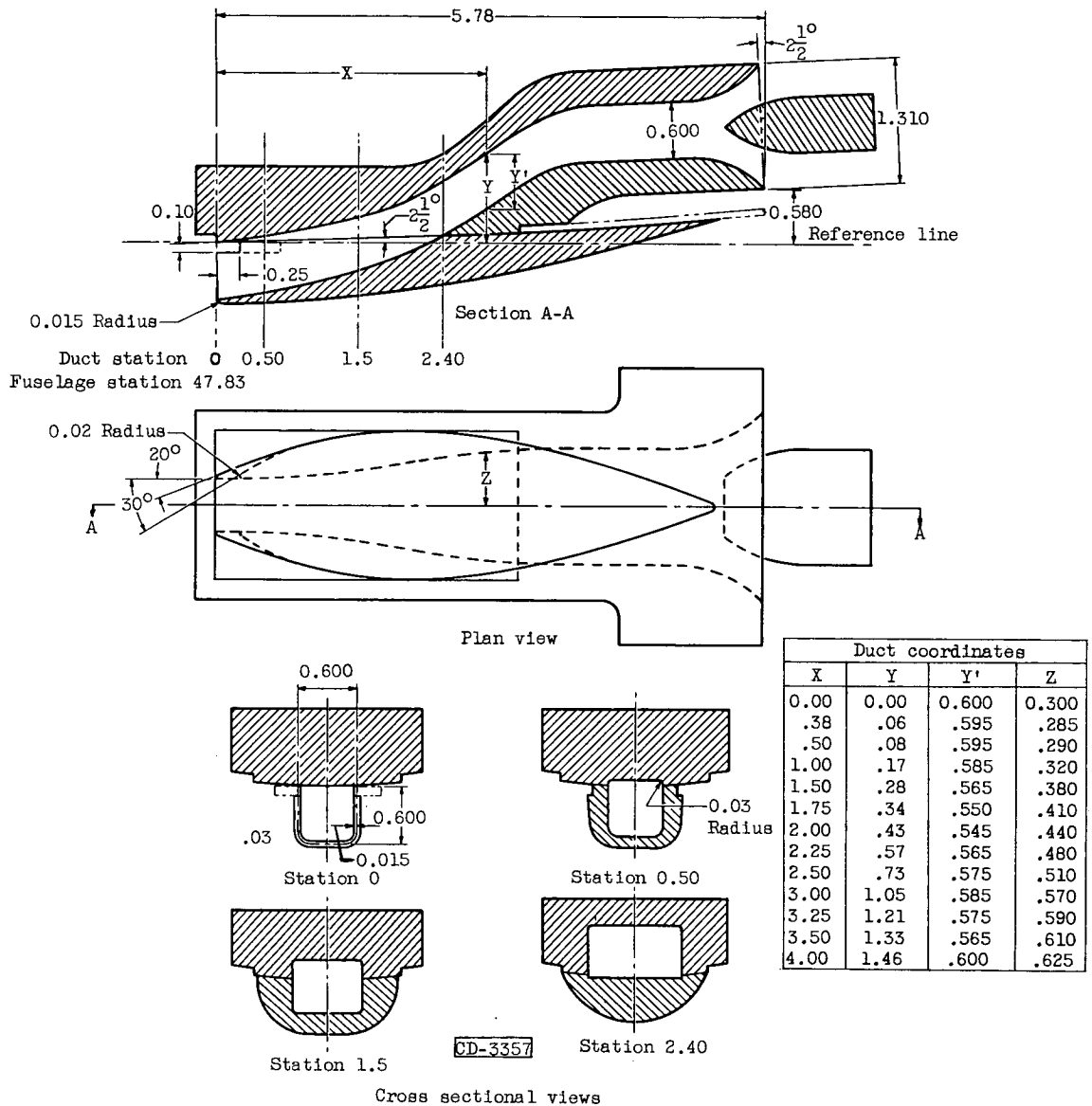


Figure 4. - Scoop inlet details. (All dimensions are in inches.)

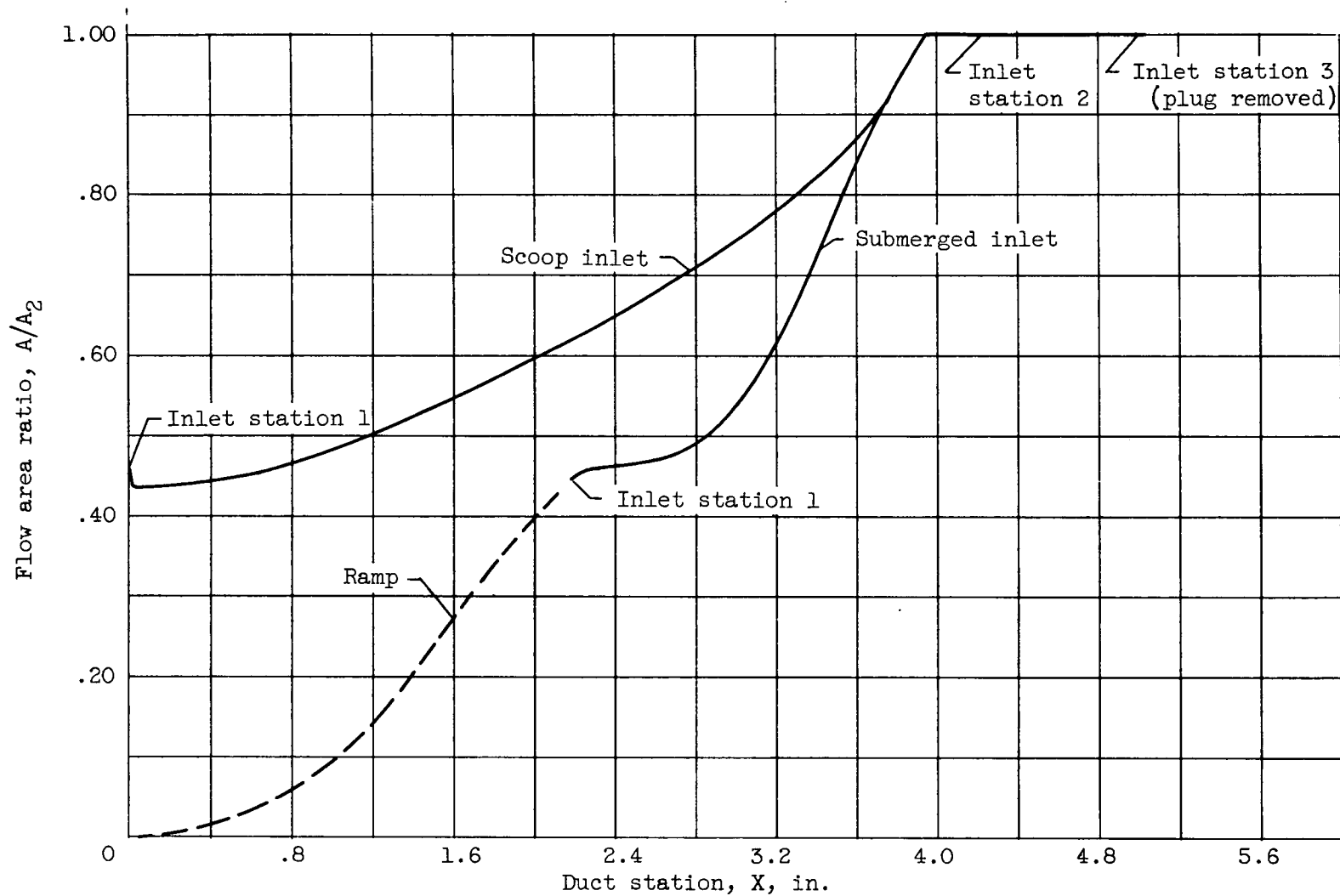


Figure 5. - Flow area variation of submerged and scoop inlets. Area of inlet station 2, A_2 , 0.750 square inch.

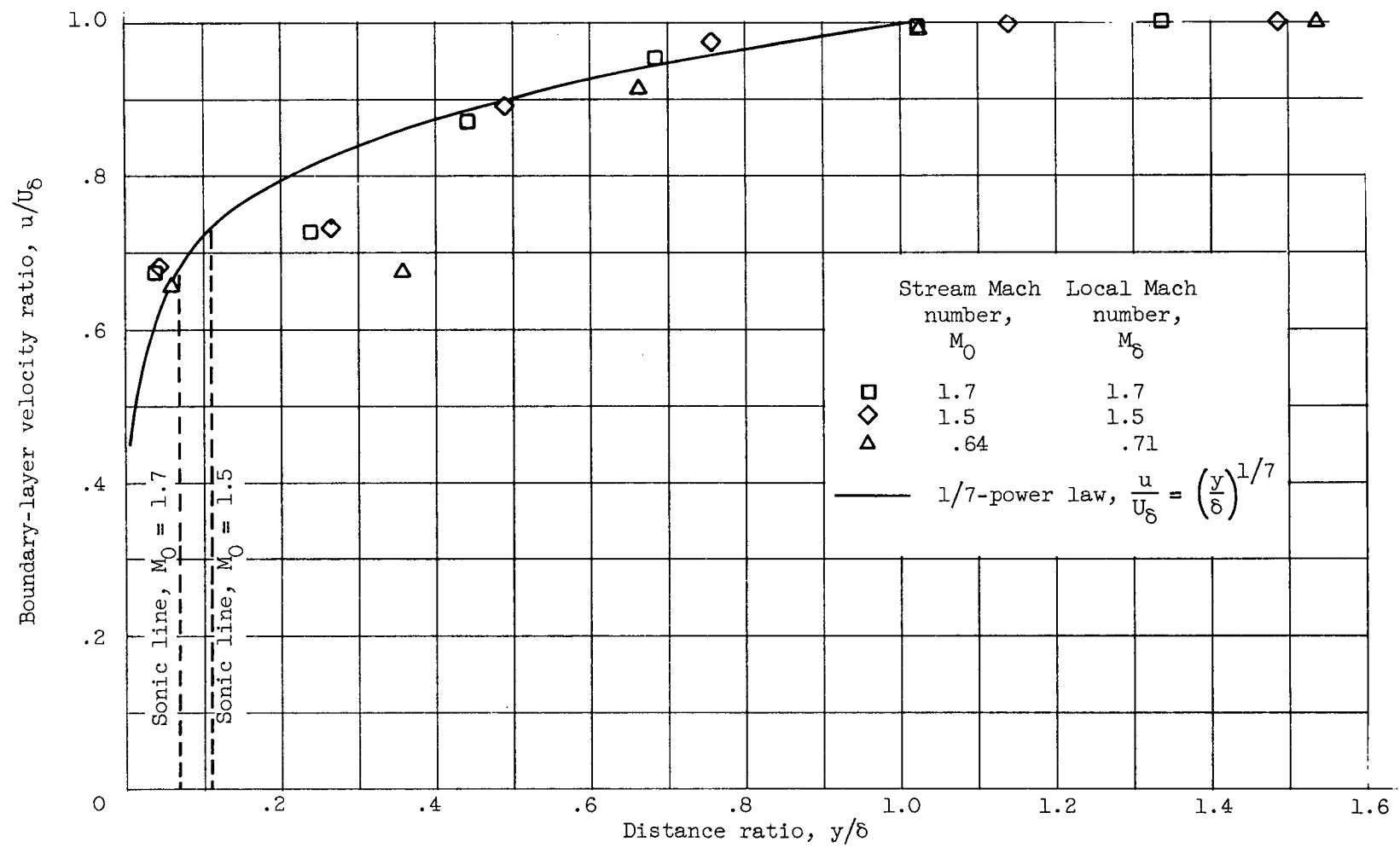


Figure 6. - Boundary-layer profiles ahead of inlets. Angle of attack, α , 0.

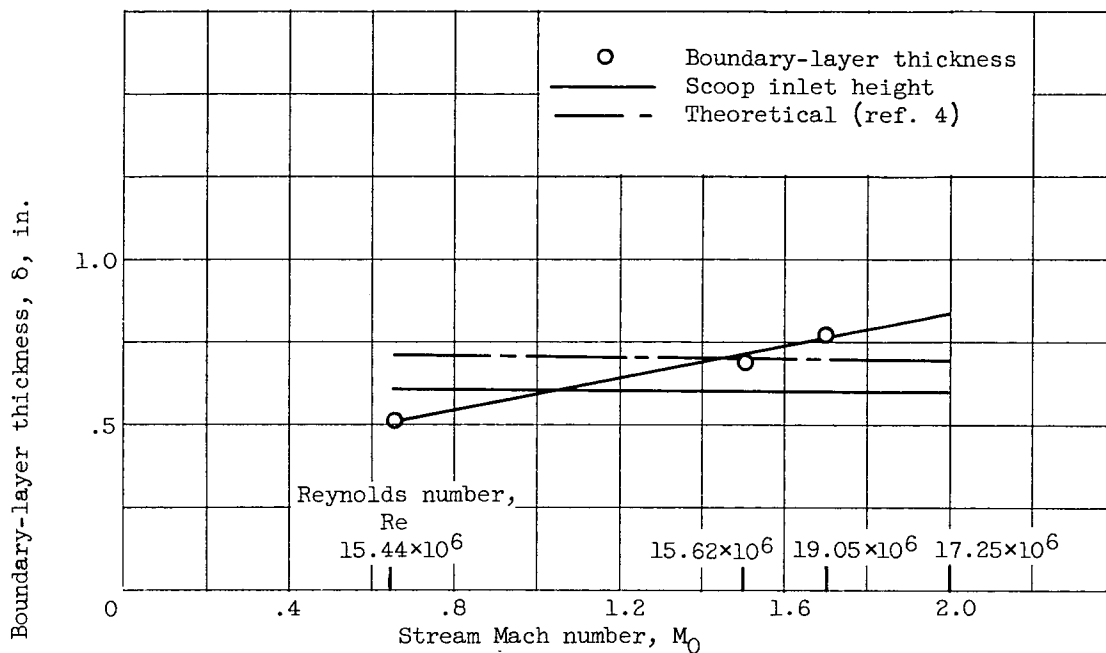


Figure 7. - Boundary-layer thickness ahead of inlets. Angle of attack, α , 0.

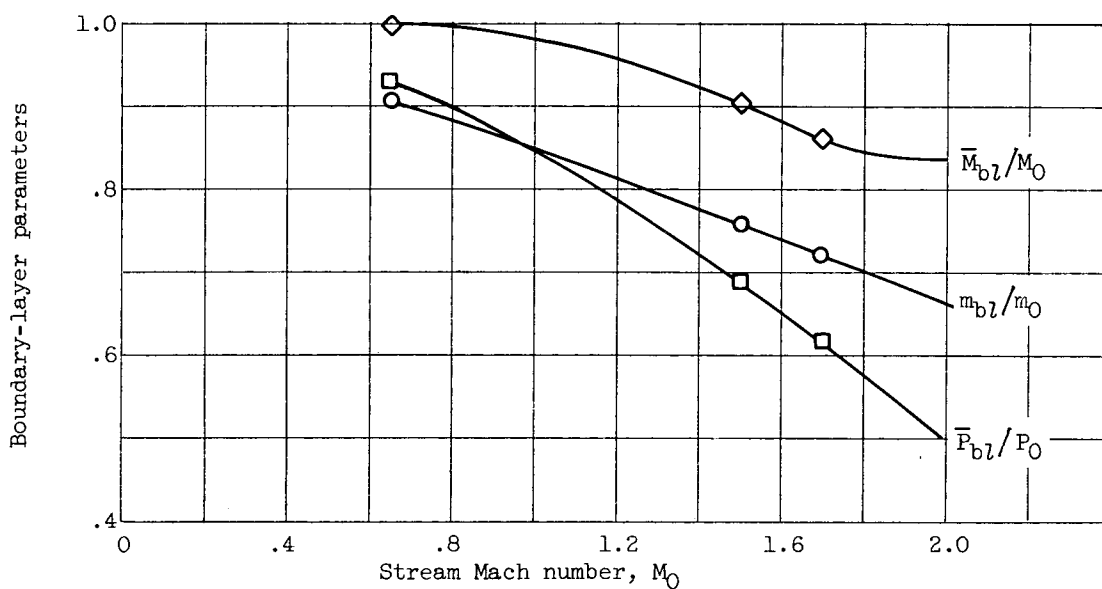


Figure 8. - Ratio of average boundary layer to free-stream parameters. Angle of attack, α , 0. (Based on scoop inlet height, a , 0.6 in.)

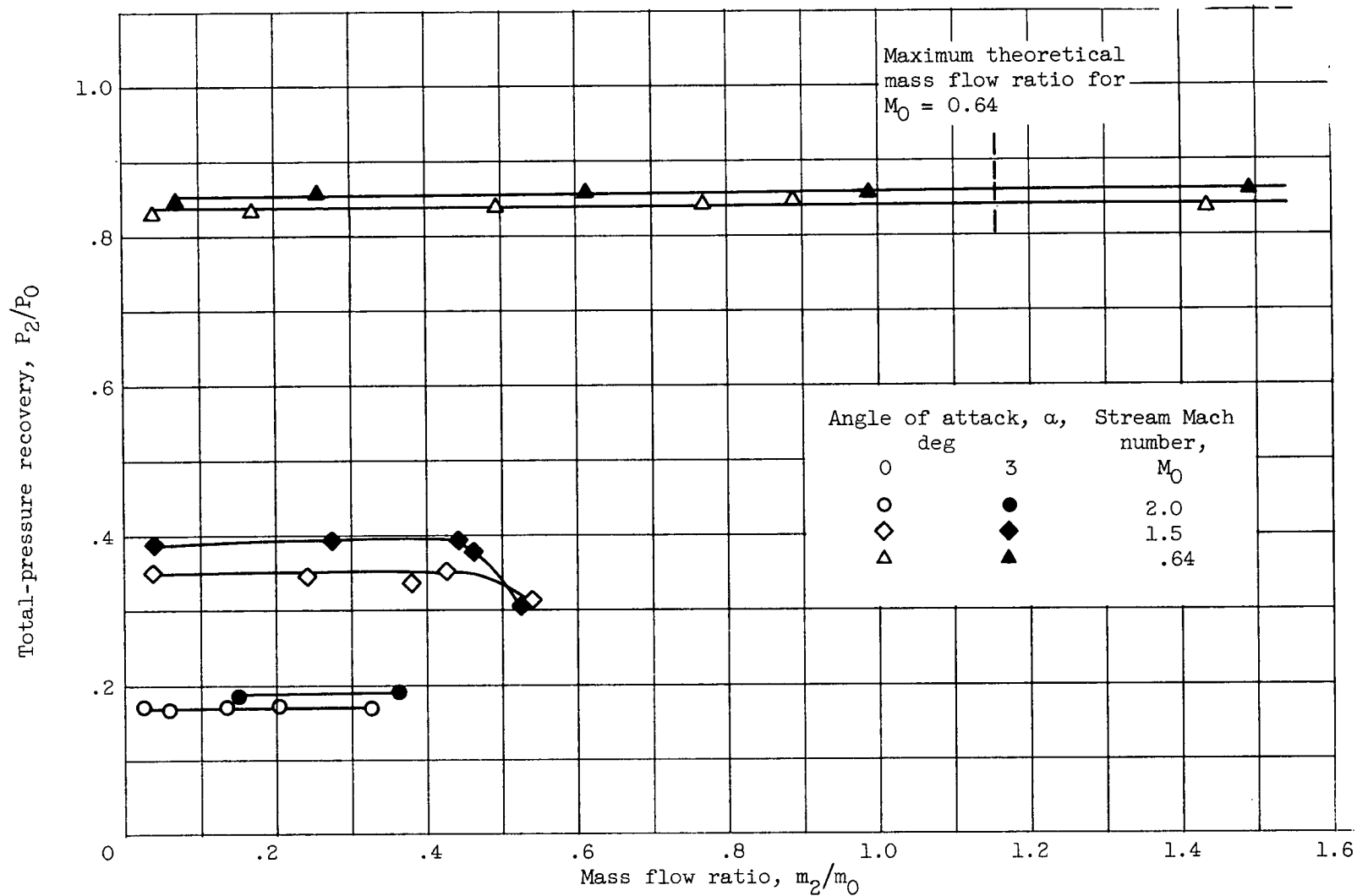


Figure 9. - Total-pressure recovery of submerged inlet.

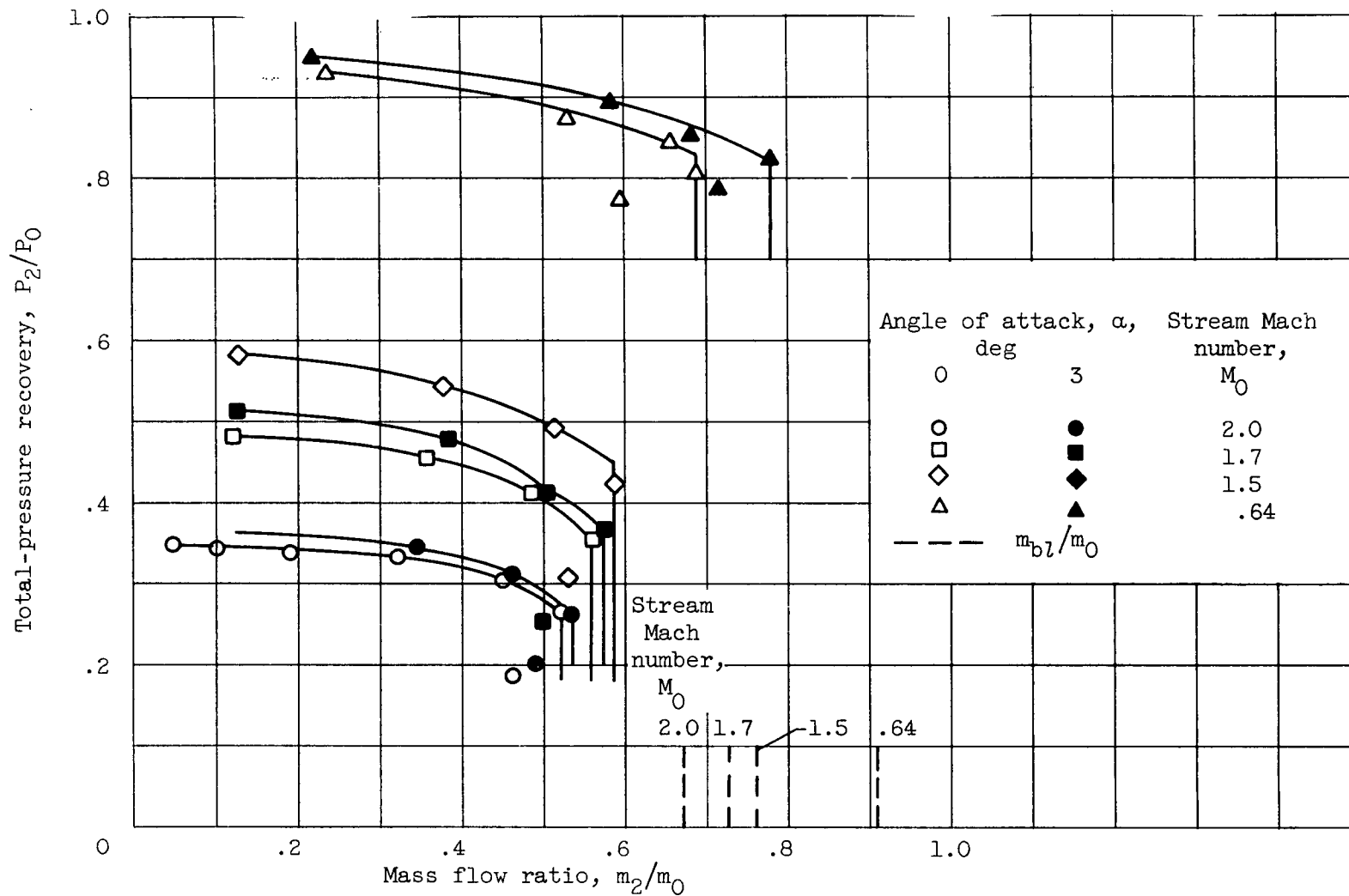


Figure 10. - Total-pressure recovery of scoop inlet.

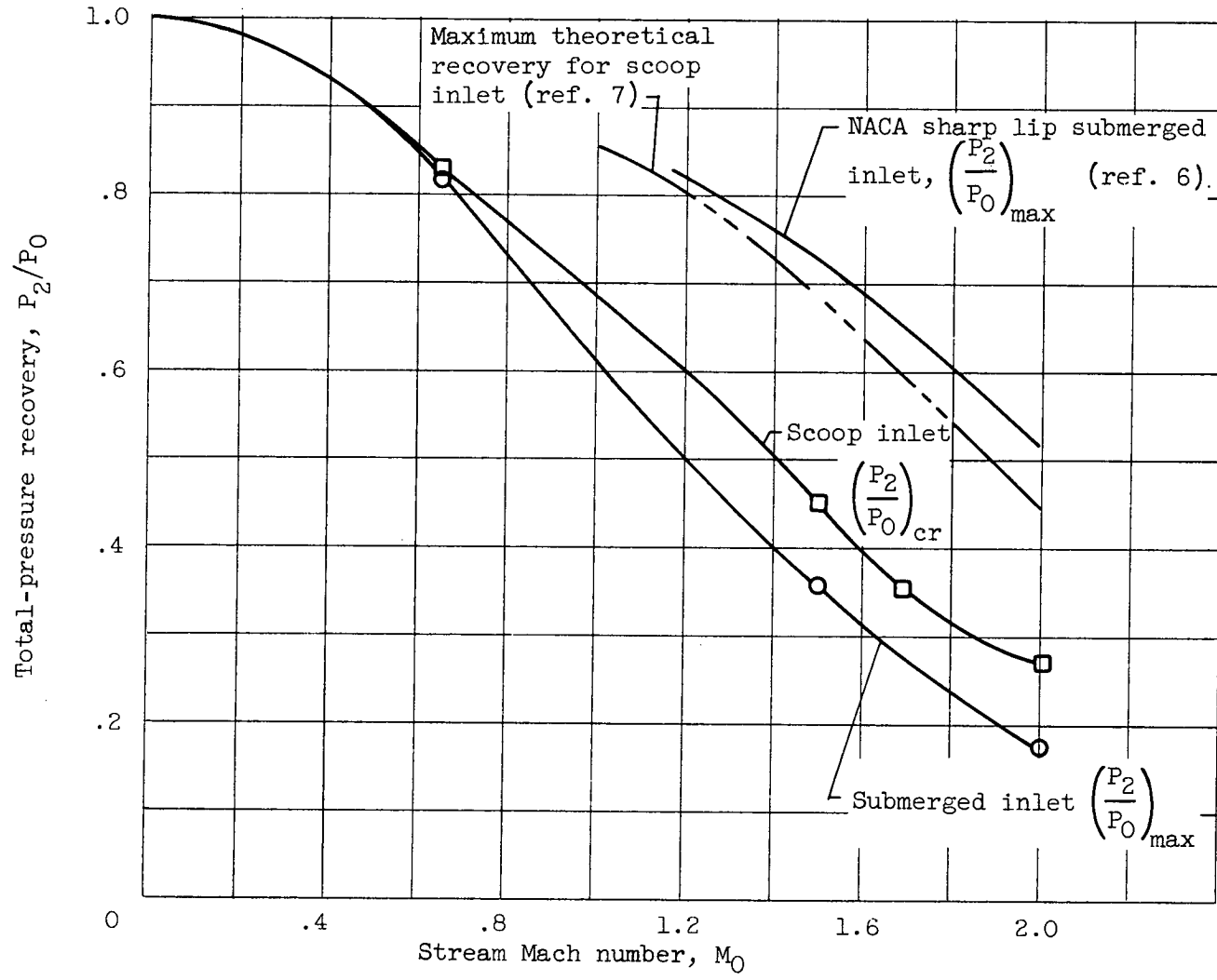


Figure 11. - Total-pressure recovery of submerged and scoop inlets. Angle of attack, α , 0.

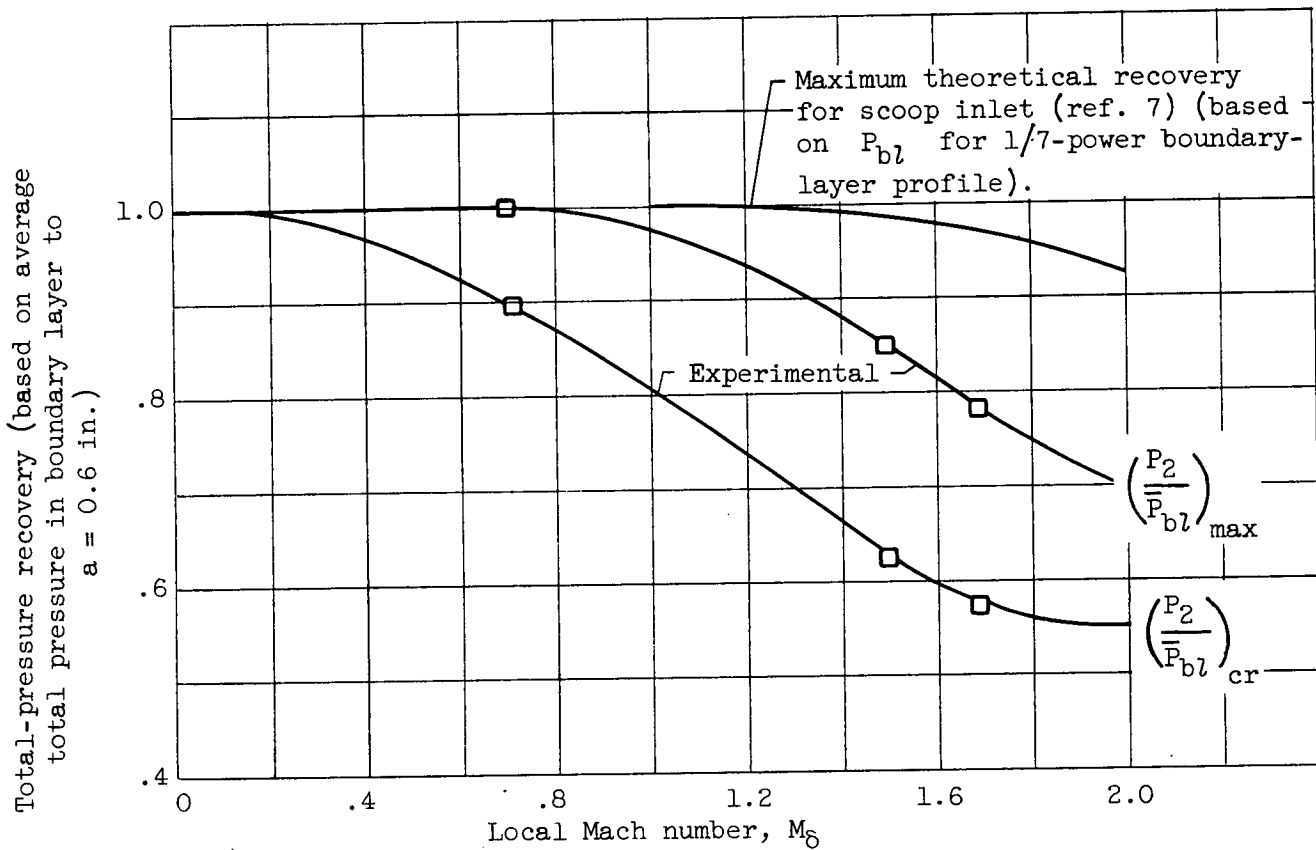


Figure 12. - Scoop inlet total-pressure recovery. Based on initial boundary-layer conditions.